

¹J. T. Anderson and A. M. Goldman, Phys. Rev. Letters **23**, 128 (1969).

²D. E. McCumber, J. Appl. Phys. **39**, 3113 (1968).

³V. Ambegaokar and B. I. Halperin, Phys. Rev. Letters **22**, 1364 (1969).

⁴Yu. M. Ivanchenko and L. A. Zil'berman, Zh. Eksperim. i Teor. Fiz. **55**, 2395 (1968) [Soviet Phys. JETP **28**, 1272 (1969)].

⁵Yu. M. Ivanchenko and L. A. Zil'berman, Zh. Eksperim. i Teor. Fiz. Pis'ma v Redaktsiyu **8**, 189 (1968) [Soviet Phys. JETP Letters **8**, 113 (1968)].

⁶More precisely, the dimensionless parameter $\beta = (2eI_1/\hbar C) R^2 C^2$, as defined in the text, is taken to be zero in Ref. 3, whereas the calculation in Ref. 5 is valid for $\beta_c \gg 1$ and $\gamma = (\hbar I_1/ekT) \gg 1$, in the region where $x = (I/I_1) < 1$. Although the experimental values of γ and β_c in Ref. 1 are obtained as a result of a two-parameter

fit (I_1 and T) with the theoretical expression due to Ambegaokar and Halperin, and hence may not be relevant for a correct theory, their orders of magnitude should be correct. These values for β_c range from 1 to 4, and γ varies between 3 and 15.

⁷See, e.g., M. C. Wang and G. E. Uhlenbeck, Rev. Mod. Phys. **17**, 323 (1945).

⁸Since time is being considered in the units of RC , in the absolute units the attempt frequency is $\omega = \beta_c^{1/2} \times (1-x^2)^{1/4}/RC$ rad/sec.

⁹S. Chandrasekhar, Rev. Mod. Phys. **15**, 1 (1943).

¹⁰This was pointed out to us by V. Ambegaokar (private communication). We are very thankful to him for his comments.

¹¹J. Kurkijarvi and V. Ambegaokar, Phys. Letters **31A**, 314 (1970).

Superconductivity of Dilute Indium-Thallium Alloys*

D. U. Gubser,[†] D. E. Mapother, and D. L. Connelly

Department of Physics and Materials Research Laboratory, University of Illinois, Urbana, Illinois 61801

(Received 15 May 1970)

Critical-field measurements, determined from isothermal magnetization curves, are reported for InTl alloys covering the concentration range of 0–7% Tl. Since In and Tl have the same number of valence electrons, the valence effects which tend to mask the effect of anisotropy in the energy gap should be minimized. Critical-field measurements down to $T = 0.35$ °K provide an accurate determination of H_0 , the critical field at $T=0$, and of γ , the temperature coefficient of the normal electronic specific heat. New values for γ ($= 1.672 \pm 0.003$ mJ/mole °K) and for H_0 ($= 281.53 \pm 0.06$ G) are reported for pure In. No effect on γ due to alloying is observed; however, changes in the quantities T_c , H_0/T_c , and $(dH_c/dT)_{T=T_c}$ are observed and are compared with the anisotropy theory of Markowitz and Kadanoff and of Clem. Significant departures from the predictions of anisotropy theory are noted for all the measured parameters.

I. INTRODUCTION

The effects of dilute nonmagnetic impurities on the superconducting properties of pure metals have been studied experimentally for some time.^{1–5} These effects are separated into two classes to distinguish those which do from those which do not depend on the particular type of impurity. The impurity-independent effects are attributed to changes in the isotropic mean free path (IMFP) of an electron^{6,7} and to changes in the anisotropy of the superconducting energy gap, Δ_k .^{8–10} The impurity-dependent effects, the so-called valence effects, are attributed to changes in the basic parameters of the metal, such as the electronic density of states. Anisotropy effects on the thermodynamic properties of superconductors are typically much smaller than valence effects and are therefore difficult to isolate and compare with theoretical predictions.

Valence effects are minimal in InTl alloys since In and Tl have the same number of valence electrons. The electron concentration n in this alloy system is

constant, and all quantities dependent on n , such as the electronic density of states, should not be affected by the additions of Tl. Therefore, InTl alloys should be particularly suitable for studying anisotropy-induced changes in superconducting properties.

II. EXPERIMENTAL TECHNIQUE

A. Apparatus

The apparatus used to measure the critical fields and critical temperatures of the samples is shown in Fig. 1. The samples were positioned inside the cryostat by supporting them in a copper sample holder which was attached to the end of a long sample rod (see Fig. 1). This sample rod could be removed to change the sample and replaced within the cryostat while the system remained at cryogenic temperatures.

For measurements below 1°K, the superconducting sample was surrounded by a bath of liquid He³ whose temperature was controlled by regulating the

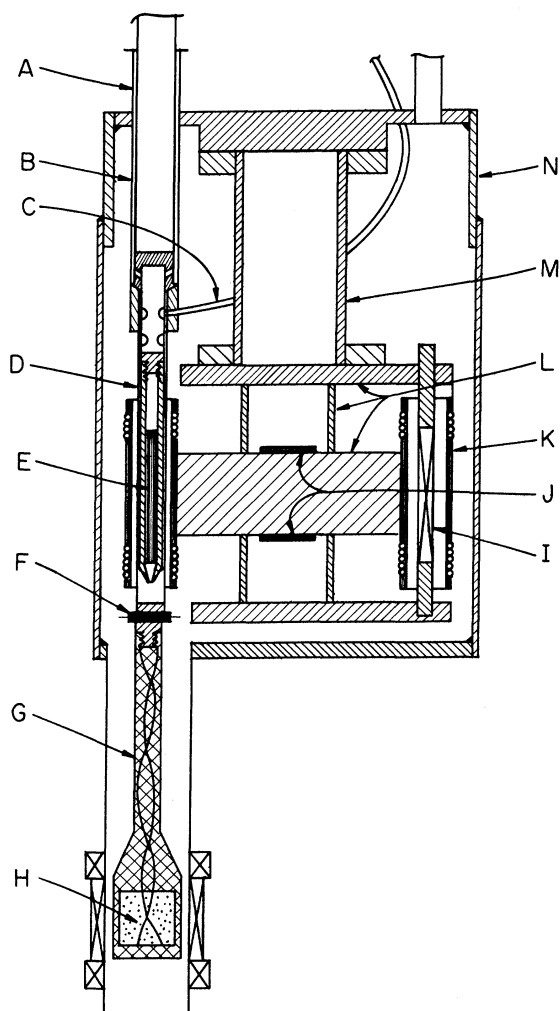


FIG. 1. A: He³ pumping line; B: removable sample support tube; C: He³ fill and vapor pressure line; D: copper sample holder; E: sample; F: Speer resistance thermometer; G: thermal link; H: CMN powder; I: solenoid; J: piezoelectric "bimorphs"; K: pick-up coil pair; L: vibrator assembly; M: vibrator mount; N: vacuum can.

pressure over the bath. The temperature was determined by measuring the resistance of a 470- Ω $\frac{1}{2}$ -W Speer carbon resistor which was in contact with the bath and was calibrated against the 1962 He³ vapor pressure scale.¹¹ Attached thermally to the bottom of the He³ chamber was some powdered cerium magnesium nitrate (CMN) salt which was used as a secondary thermometer for calibrating the Speer resistor in the temperature range below 1°K. For measurements in the vicinity of T_c , exchange gas was introduced into the vacuum can and sample chamber, and the temperature was controlled

by regulating the pressure over the outer He⁴ bath. In this region the Speer resistor was calibrated against the 1958 He⁴ vapor pressure scale.¹²

Isothermal magnetization measurements of the superconducting samples were made with a null magnetometer consisting of two symmetrical pairs of pick-up coils mounted on a piezoelectric vibrator¹³ (see Fig. 1). The signal induced by the superconducting sample in one pair of vibrating coils was cancelled by an automatically regulated current through a small solenoid mounted on the axis of the second vibrating coil pair. The solenoid current necessary to produce the null reading is proportional to the sample magnetization.

A signal induced in the vibrating pick-up coils — due to unbalance between the magnetic moments of the sample and the small solenoid — is fed directly to a lock-in amplifier (Princeton Applied Research Laboratory, Model HR-8). This amplifier, which also generates the driving voltage for the vibrator, selectively amplifies the input signal of the proper frequency (230 Hz) and phase. The rectified signal output of the amplifier is fed into an electronic integrator whose output voltage is therefore proportional to the integrated signal from the pick-up coils. This voltage controls the current in the small solenoid and compensates for any difference between the magnetic moments of the sample and the solenoid.

The magnetic field applied to the sample was produced by an aluminum-foil-wound nitrogen-cooled solenoid designed at the University of Illinois and built by Ogallalla Electronics Manufacturing Inc., Ogallalla, Neb. The high conductor density and favorable cooling conditions which are possible in the foil-wound technique of construction provide a magnetic field of 3000 G within a 4 in. diam at an input power of about 1 kW. The field at the sample was measured with an accuracy of about 1 part in 10⁴, and was homogeneous to about 1 part in 10³ over the sample's length.

The rate of change of the applied magnetic field affects the determination of H_c in two ways. Eddy current heating in the metal parts of the cryostat and in normal regions of the specimen create temperature uncertainty if the field sweep rate is too fast. A separate consideration is that a finite time is required for redistribution of magnetic flux within the volume of the superconducting specimen in response to changes in the applied field. Both effects require that observations be made at slow and constant field sweep rates, although in practice the time constant for flux motion was the limiting consideration.

A very stable rate controller was constructed to meet this requirement. The controller permitted linear field sweeps of as low as 10⁻³ G/sec and could

hold at any field value for extended periods (drift $\approx 10^{-3}$ G/min). An acceptable value of field sweep rate was determined by stopping a sweep in the middle of the transition and waiting for a minute or longer. If no change in the sample's magnetization occurred, it was assumed that the sample was undergoing a quasistatic transition. For the samples used in this experiment, sweep rates of 10^{-2} G/sec or slower were necessary to achieve reproducible transitions.

B. Samples

Cylindrical polycrystalline samples ($1\frac{1}{4} \times \frac{1}{16}$ in. diam) were prepared by thoroughly mixing desired ratios of In and Tl in the molten state. The resulting alloy was cooled and swaged to the final diameter and then annealed at 135°C in $\frac{1}{2}$ atm of hydrogen for 4 days.

The residual resistance ratio

$$\rho_r = R_{4.2}/(R_{273} - R_{4.2}), \quad (1)$$

where R_T is the electrical resistance at a temperature T of the samples, obeyed a quadratic relationship (Nordheim's rule) with Tl concentration x (x is the molar fraction of Tl atoms),

$$\rho_r = 2.35x(1-x). \quad (2)$$

The rms scatter of the experimental points from this relationship was less than 0.0003. This excellent agreement with Nordheim's rule provides an indication that the normal-state parameters, such as atomic volume, crystal structure, and number of free electrons, change very little in this alloy system.¹⁴

The Ginzburg-Landau parameter κ increases with Tl concentration according to the Goodman relation¹⁵

$$\begin{aligned} \kappa &= \kappa_p + 7.5 \times 10^3 \gamma^{*1/2} \rho \\ &= \kappa_p + 7.5 \times 10^3 \gamma^{*1/2} \eta [x(1-x)], \end{aligned} \quad (3)$$

where κ_p is the value characteristic of pure host metal; γ^* is the temperature coefficient of normal electronic specific heat per cm^3 ; ρ is the residual resistivity (Ω/cm^2); n is the constant of proportionality between ρ and $x(1-x)$.

At about 5% Tl, the κ value of the alloy becomes large enough ($\kappa > 1/2.4$) to cause the formation of a superconducting surface sheath on the sample. The sheath forms because the lattice periodicity is disrupted at the sample's surface and it persists until the critical field H_{c3} ($H_{c3} = 2.4\kappa H_c$) is reached.¹⁶ For $\kappa < 1/2.4$, H_{c3} corresponds to a supercooling field and for $\kappa > 1/2.4$, H_{c3} corresponds to the field at which all traces of superconductivity vanish. When $H_{c3} > H_c$, surface superconductivity partially shields the applied field from the bulk of the super-

conductor creating hysteretic transitions which obscure the precise determination of H_c .¹⁷

Since the superconducting surface sheath is caused by the boundary conditions imposed at the surface of the sample, changing the conditions on the sample's surface should affect the sheath. A reduction in the shielding effect of the surface sheath for samples coated with copper has been reported.¹⁸ This reduction is presumably due to the proximity effect in the normal metal-superconductor boundary. The complete elimination of the surface sheath has also been reported for samples coated with Ni and Cr.¹⁸ This complete elimination is thought to be caused by the magnetic properties of Ni and Cr.

The samples used in this study were coated with a thin ($\approx 500 \text{ \AA}$) layer of Mn to eliminate hysteretic transitions in the high-concentration alloys ($x \geq 5\%$). As with Ni and Cr, it has previously been observed that Mn stops surface sheath superconductivity.¹⁹

III. RESULTS

A. Data Analysis

A typical magnetization curve for the alloy system is shown in Fig. 2. Supercooling and incomplete expulsion of flux at the supercooling transition were common to all samples. This trapped flux is expelled erratically as the applied field is reduced until the sample returns to the Meissner ($B=0$) state at a point above zero applied field.

Transitions were observed after cycling the samples through H_c and back through the supercooling field. The initial magnetization of a sample was not always reproducible because of varying amounts of trapped flux; however, the linear intermediate-state portion of the transition was reproducible to within the width of the recorder trace. The value of H_c was determined by extrapolation of the magnetization curve to $M=0$ (as shown in Fig. 2) and was not affected by varying amounts of trapped flux.

Both coated and uncoated In samples were measured to determine if the Mn coating had any effect on the bulk superconducting properties. No change was noted in the H_c determination; however, at low temperatures, the supercooling field of the coated sample was about 3% lower than that of the uncoated sample. This is an expected result since nucleation at the surface of the sample is inhibited by the Mn coating.

The critical-field data below 1°K were fitted by a least-squares analysis to the thermodynamic relation²⁰

$$H_c^2 = H_0^2 - (4\pi\gamma/V)T^2, \quad (4)$$

where $H_0 = H_c(T=0)$, V is the molar volume, and γ is the temperature coefficient of normal electronic specific heat. This relation is valid at low temper-

atures where the superconducting electronic entropy is negligible.

Table I gives a comparison of the experimentally derived superconducting properties of pure In with the earlier work of Finnemore and Mapother (FM).²⁰ H_0 and γ/V were determined from the coefficients of (4); T_c and $(dH_c/dT)_{T=T_c}$ were derived from the critical-field data near T_c . All quantities measured are consistent with the earlier work of FM except for H_0 .

FM report a value of $\gamma = 1.66$ mJ/mole °K with an accuracy of 0.8% while an analysis of the data from this work gives $\gamma = 1.672$ mJ/mole °K with an accuracy of 0.2%. The error limits of the two values overlap but the value of this work is believed to represent an improvement in the γ determination. The calorimetric γ value of O'Neal and Phillips²¹ ($\gamma = 1.69$ mJ/mole °K) is slightly higher than that allowed by the error limits of either the FM value or the value of this work, and the calorimetric value of Bryant and Keesom²² ($\gamma = 1.61$ mJ/mole °K) is considerably lower.

In trying to resolve the discrepancy in H_0 , the

aluminum magnet used to produce the applied field was twice calibrated, and no significant change in the coil constant was found. Critical-field measurements were repeated on the same sample used by FM and again an H_0 of 281.53 G was observed. As a final check, the sample was placed in a He³-He⁴ dilution refrigerator and its critical field measured at a temperature of approximately 40 mdeg. Once again an H_0 of about 1 G lower than FM was seen. It is therefore believed that the value of $H_0 = 281.53$ G is more reliable than the previously quoted value.

B. Impurity Effects

Table II gives a compilation of the various experimental quantities determined in this work for dilute InTl alloys.

A plot of T_c versus x and of H_0 versus x is given in Fig. 3 and shows some of the typical characteristics of impurity doping. These features are the initial decrease in the curves due to a reduction of the effective anisotropy in the material and the more gradual change at higher concentrations due

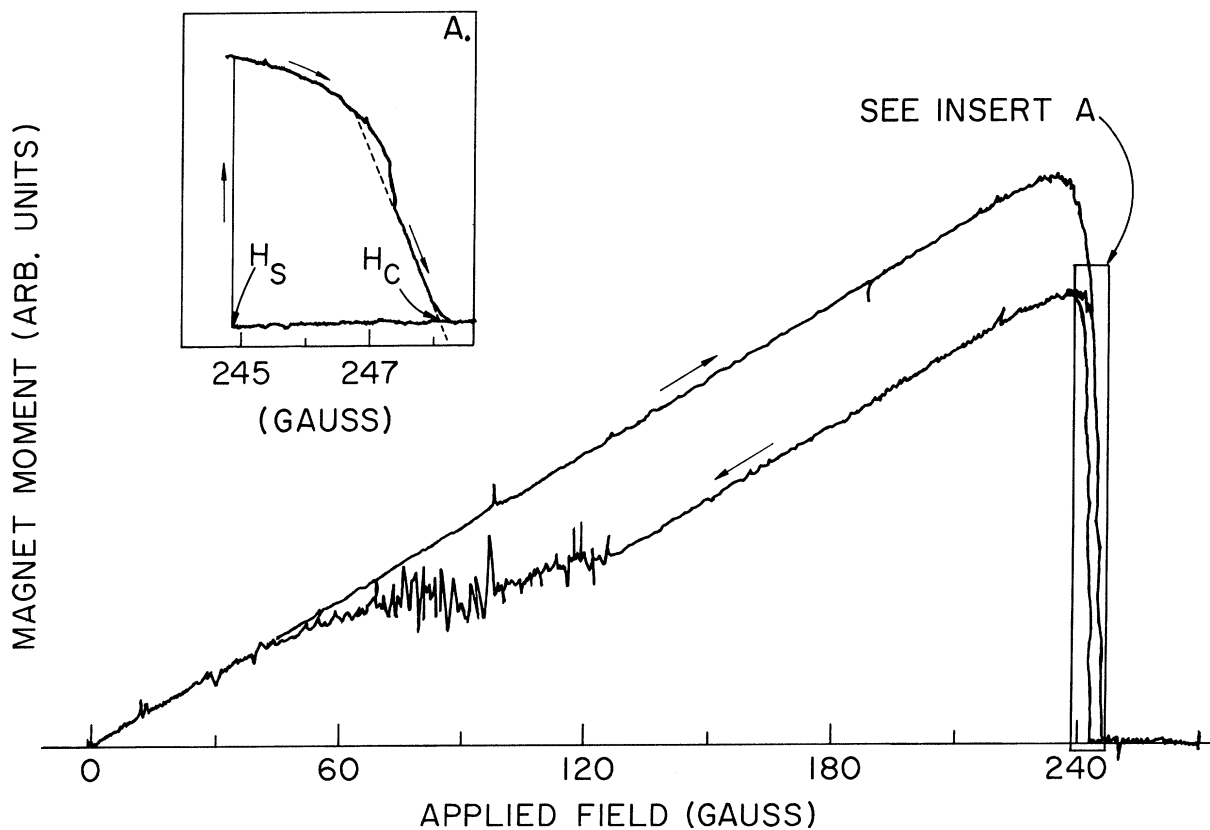


FIG. 2. Typical magnetization curve for the InTl alloy. This curve was obtained from the 4% Tl sample at a temperature below 1 °K. The method of determining H_c is shown in the insert.

TABLE I. Characteristic superconducting parameters of In.

| | Quantity | This work | FM |
|---------------------|--------------------------|--------------------|--------------------|
| T_c | deg | 3.4087 ± 0.001 | 3.4070 ± 0.001 |
| H_0 | G | 281.53 ± 0.06 | 282.66 ± 0.12 |
| γ | mJ/mole deg ² | 1.672 ± 0.003 | 1.659 ± 0.012 |
| $(dH_c/dT)_{T=T_c}$ | G/deg | -155.4 ± 1 | -155.6 ± 1 |

to IMFP effects (presumably valence effects are small in this alloy system). However, there is a peculiar feature in these curves.

Between 1.0 and 1.5% Tl ($\rho_r = 0.02$ to 0.03), there is a noticeable downturn in the curves which is very prominent in the H_0 plot and also observable in the T_c plot. This feature was first noted in the T_c curve by Merriam, Hagen, and Luo.⁵ It has not been observed in other alloy systems, but seems characteristic of the InTl system.

1. Critical Temperatures

In the weak coupling limit, Markowitz and Kadanoff⁹ (MK) calculated critical temperature changes due to a reduction of the effective gap anisotropy. Their result is given by the expression

$$\Delta T_c / T_c = \langle a^2 \rangle I_c(\chi), \quad (5)$$

where

$$I_c(\chi) = \int_0^{2\beta_c \omega_D / \chi} \frac{dy}{y} \frac{\tanh(\frac{1}{4}\chi y)}{1+y^2}$$

and

$$\langle a^2 \rangle = \langle (\Delta_k - \langle \Delta_k \rangle)^2 / \langle \Delta_k \rangle^2 \rangle.$$

χ is a theoretical parameter which is related to the residual resistance ratio of the material by

$$\chi = \alpha^i \theta \rho_r, \quad (6)$$

where α^i is a constant of order unity and θ is a

constant dependent on the host material only.

In the theory of MK, changes in T_c due to the IMFP effect and the valence effect are lumped together into one term which varies linearly with $\chi(\rho_r)$. The complete expression for impurity-induced changes in T_c is thus

$$T_c = K^i \chi + \langle a^2 \rangle T_c I_c(\chi), \quad (7)$$

where K^i is an impurity-dependent constant.

MK and also Ginsberg⁶ show that (7) is conveniently approximated for $1 < \chi < 100$ by the expression

$$\Delta T_c = A \rho_r + B \rho_r \ln \rho_r, \quad (8)$$

where

$$A = \{ K^i + \langle a^2 \rangle T_c [-0.36 + 0.078 \ln(\alpha^i \theta)] \} \alpha^i \theta,$$

$$B = 0.078 \langle a^2 \rangle T_c \alpha^i \theta.$$

Clem¹⁰ has also shown that for small χ (i. e., $\chi < 1$), (7) is given by the expression

$$\frac{\Delta T_c}{\rho_r} = (0.393 \langle a^2 \rangle T_c + K^i) \theta \alpha^i + 0.535 \langle a^2 \rangle T_c (\theta \alpha^i)^2 \rho_r. \quad (9)$$

Using $\theta = 140$, as given in MK's paper, and $\alpha^i = 1$, one obtains from (6)

$$\chi = 140 \rho_r. \quad (10)$$

The logarithmic expression for $\Delta T_c / \rho_r$, (8), should

TABLE II. Observed parameters of In-Tl alloys.

| x (%) | $10^2 \rho_r$ | T_c (°K) | H_0 (G) | γ^* (mJ/cm ³ deg ²) | $(dh/dt)_{t=1}$ |
|------------|---------------|---------------|--------------|--|-----------------|
| 0 | 0.0112 | 3.4087 | 281.53 | 0.1088 | -1.882 |
| 0.2000 | 0.4850 | 3.4017 | 281.25 | 0.1087 | -1.860 |
| 0.6006 | 1.4140 | 3.3896 | 280.93 | 0.1089 | -1.902 |
| 1.0034 | 2.343 | 3.3796 | 280.41 | 0.1087 | -1.869 |
| 1.505 | 3.504 | 3.3629 | 278.98 | 0.1089 | -1.867 |
| 1.992 | 4.617 | 3.3422 | 277.08 | 0.1088 | -1.870 |
| 2.502 | 5.755 | 3.3253 | 275.67 | 0.1087 | -1.861 |
| 2.988 | 6.843 | 3.3140 | 274.82 | 0.1090 | -1.860 |
| 3.491 | 7.929 | 3.3076 | 274.09 | 0.1090 | -1.850 |
| 4.007 | 9.066 | 3.3008 | 273.73 | 0.1096 | -1.840 |
| 4.481 | 10.07 | 3.2974 | 273.32 | 0.1087 | -1.828 |
| 5.048 | 11.20 | 3.2929 | 272.97 | 0.1088 | -1.819 |
| 6.763 | 14.80 | 3.2830 | 272.41 | 0.1088 | -1.804 |

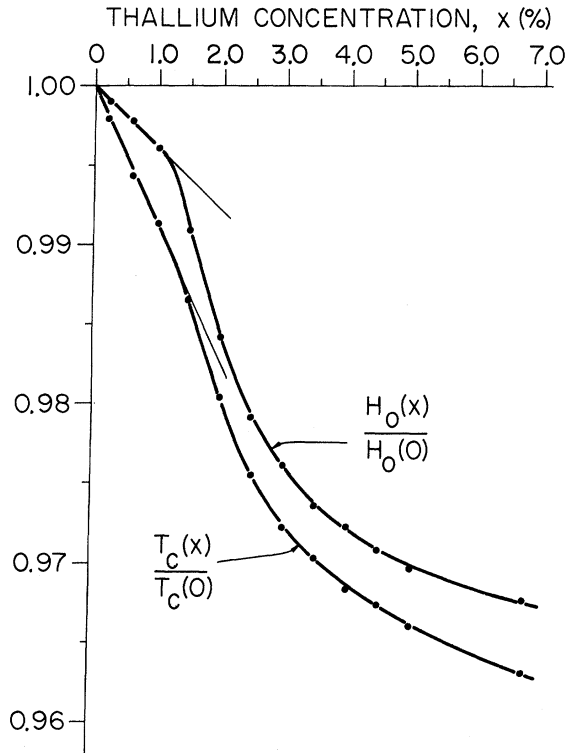


FIG. 3. Variation of T_c and H_0 as a function of Tl concentration. All data are normalized by the corresponding values for pure In ($x=0$). The straight lines through the low-concentration data emphasize the peculiar drop in both curves which occurs between 1.0 and 1.5% Tl. Error limits of these data are within the size of the plotted points.

therefore be valid over the residual resistivity range $0.007 < \rho_r < 0.7$, while below $\rho_r \approx 0.007$, (9) should apply. All of the data from this work, except the lowest impurity point, fall within the range of the logarithmic approximation.

Figure 4 shows a plot of $\Delta T_c / \rho_r$ versus $\ln \rho_r$ for the InTl system. For $\rho_r > 0.06$, the data do obey a logarithmic relationship, but for $\rho_r < 0.06$, there is a noticeable deviation from the expected behavior. Also shown in the same plot are data reported previously by other workers. Although there are slight differences among the data, the results show substantially the same features, i. e., a noticeable decrease in $\Delta T_c / \rho_r$ between the residual resistance values of $\rho_r \approx 0.025$ to $\rho_r \approx 0.05$, and a logarithmic increase in $\Delta T_c / \rho_r$ for $\rho_r > 0.06$. It is therefore well established that the dip in the $\Delta T_c / \rho_r$ versus $\ln \rho_r$ curve is characteristic of the InTl alloy system and is not due to spurious sample defects.

Setting $\alpha^i = 1$, and using the linear portion of the $\Delta T_c / \rho_r$ versus $\ln \rho_r$ plot ($\rho_r > 0.06$), the mean-squared value of the anisotropy, $\langle a^2 \rangle$, was calculated from

(8). The result of this calculation yields

$$\langle a^2 \rangle = 0.0185, \quad (11)$$

which agrees well with the earlier estimate of MK, $\langle a^2 \rangle = 0.02$, based on an analysis of InSn and InPb data.

In their analysis of the InSn and InPb alloy systems, MK used the value $\alpha^i = 1$, as is done for the InTl system in this work. However, from the data then available on InTl alloys,³ MK were forced to assume that $\alpha^i = 0.4$ for this system in order to obtain a value for $\langle a^2 \rangle$ consistent with their analysis of the InSn and InPb systems. From more recent data⁵ and this work it appears that the earlier data³ exist in a low-concentration range where the validity of the anisotropic predictions for InTl are suspect and that the value of $\alpha^i = 0.4$ is not reliable.

Merriam *et al.*, who first noticed the dip in the $\Delta T_c / \rho_r$ data, suggest that "Brillouin-zone effects" may be the cause of the anomalous features. Brillouin-zone effects are due to electron-phonon interactions which occur as the Fermi surface of the metal approaches, touches, or overlaps the Brillouin zone of the crystal lattice.²³ Such an interaction has an effect on T_c of a superconductor due to variations in the density of electronic states at the Fermi surface, $N(0)$, or the electron-electron interaction potential V_0 .

The InTl system was chosen specifically as one in which the density of states would not change with Tl concentration; however, since the size of the Tl atom is larger than that of the In atom, the crystalline lattice structure of the alloy expands slightly

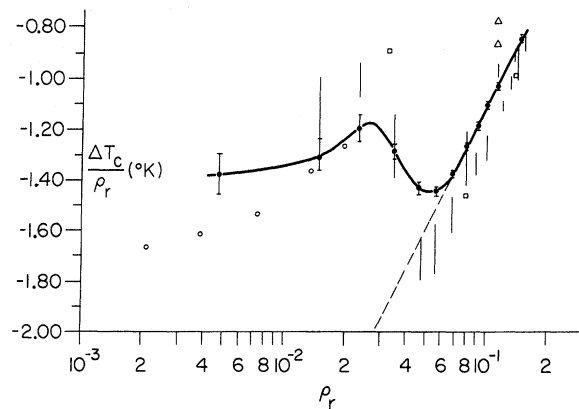


FIG. 4. Changes in the critical temperature divided by the residual resistivity, $\Delta T_c / \rho_r$, of InTl alloys as a function of $\ln \rho_r$. The dashed line shows the behavior predicted by MK (Ref. 9) for a mean-squared anisotropy value of $\langle a^2 \rangle = 0.0185$. Data from other works are shown for comparison. (Chanin, Lynton, and Serin, Ref. 3; Connell, Ref. 4; Stout and Guttman, Ref. 1; Merriam, Hagen, and Luo, Ref. 5; and this work.)

with Tl concentration. The increase in the lattice parameters, as measured by Meyerhoff and Smith,²⁴ is linear with concentration up to the crystalline phase change at 20% Tl, where the face-centered tetragonal (fct) In structure changes into a fcc structure. There is therefore a slight shift in the Brillouin zone relative to the Fermi surface.

If the Fermi surface of In is approximated by the free-electron model,^{25,26} small changes in the lattice parameters which change the Brillouin zone should have little effect on $N(0)$. However, an experimental determination of $N(0)$ for all the alloys was considered vital in order to determine if Brillouin-zone effects were present in the alloy system.

The molar volume of InTl alloys increases linearly with Tl concentration ($\Delta V/V \approx 0.1x$),²⁴ therefore, the coefficient of normal electronic specific heat [$\gamma = \frac{2}{3}\pi^2 k_B^2 N(0)V$] will correspondingly increase. Experimentally, however, the quantity determined from the low-temperature critical-field data is $\gamma/V (= \gamma^*)$ which is directly proportional to $N(0)$ and therefore should remain nearly constant. Any variation in $N(0)$, brought about by Brillouin-zone interactions, would show up in γ^* according to the relation

$$\Delta\gamma^*/\gamma^* = \Delta N(0)/N(0). \quad (12)$$

The variation of $N(0)$ also produces a change in T_c according to the relation⁷

$$\frac{\Delta T_c}{T_c} = \frac{1}{N(0)V_0} \frac{\Delta N(0)}{N(0)}. \quad (13)$$

For In, $1/N(0)V_0$ is about 3.5; therefore, the critical temperature is about 3.5 times more sensitive to a change in $N(0)$ than is γ^* . A change in $N(0)$ corresponding to a ΔT_c of 0.020°K, will produce a relative change in γ^* of only 0.2%.

Experimentally, no noticeable variation in γ^* was observed over the entire alloy range. The γ^* values were within 0.2% of the value quoted for pure In. It must be recognized, however, that the observed critical temperature deviations from anisotropy predictions are at most about 0.020°K, and if these deviations were due entirely to density-of-state changes, the corresponding change in γ^* would be about the same magnitude as the error in the γ^* determination. It is apparent that without the high accuracy in the γ^* values determined from this experiment, there would have been no hope of detecting $N(0)$ changes. Although Brillouin-zone effects cannot be completely ruled out on the basis of these data, the fact that no variational trend in γ^* was detected suggests that one look elsewhere for the cause of the strange T_c behavior in InTl.

2. Critical Fields

Clem¹⁰ rederived the original MK result for an-

isotropy-induced changes in the critical temperature of a superconductor and extended the calculation to predict changes in the critical field of a weak coupling superconductor. As previously mentioned, impurity-induced changes in the critical fields, as well as in the critical temperatures, are caused not only by anisotropy effects, but also by IMFP effects and valence effects. In the weak coupling limit, however, the ratios $VH_0^2/(8\pi\gamma T_c^2)$ ($= \tilde{H}_0^2$) and $(T_c/H_0) \times (dH_c/dT)_{T=T_c} [= (dh/dt)_{t=1}]$, where h and t are the reduced critical field and critical temperature, respectively] are free from these unwanted effects.

Clem calculated the anisotropy-induced changes in these ratios and expressed the results in the following form:

$$\frac{\Delta \tilde{H}_0(\lambda)}{\tilde{H}_0(0)} = \left(\frac{\tilde{H}_0(\lambda) - \tilde{H}_0(0)}{\tilde{H}_0(0)} \right) = \langle a^2 \rangle \delta_H(\lambda), \quad (14)$$

$$\frac{\Delta [(dh/dt)_{t=1}]}{[(dh/dt)_{t=1}]_{t=1}} = \left(\frac{(dh/dt)_{t=1} - (dh/dt)_{t=1}}{(dh/dt)_{t=1}} \right)_{t=1} = \langle a^2 \rangle \delta_h(t, \lambda)_{t=1}, \quad (15)$$

where the functions $\delta_H(\lambda)$ and $\delta_h(t, \lambda)$ are mathematical expressions defined in Clem's paper. The parameter λ in these expressions is related to χ (and to ρ_r) of the MK theory by the relation

$$2\pi\lambda = \chi = a^t \theta \rho_r. \quad (16)$$

Using the value $\langle a^2 \rangle = 0.0185$, obtained from the ΔT_c data, the theoretical changes in the quantity \tilde{H}_0 as a function of ρ_r are calculated and shown in Fig. 5 along with the experimental determinations of this ratio. As in the case of the ΔT_c data, the weak coupling anisotropic predictions do not explain the observed behavior. The lowest two or three points, $\rho_r \lesssim 0.02$, seem to be in reasonable agreement with

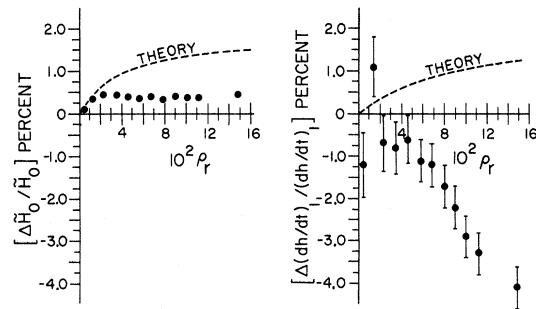


FIG. 5. Percent change in the functions \tilde{H}_0 and $(dh/dt)_{t=1}$, defined in (14) and (15), as a function of the residual resistivity ρ_r . The dashed lines on the plots are theoretical predictions of Clem (Ref. 10) using a mean-squared anisotropy value of $\langle a^2 \rangle = 0.0185$.

theory, but all higher residual resistance points fall well off the theoretical curve.

The surprising feature of this curve is not that deviations from anisotropy theory occur, because deviations also are seen in the T_c data, but that the data above $\rho_r = 0.02$ are unexplained in terms of anisotropy. The ΔT_c data appear to be in good agreement with anisotropy theory for large ρ_r , but the \bar{H}_0 data within the same ρ_r range deviate significantly from the theory.

Figure 5 also shows the calculated and experimental changes in the ratio $(dh/dt)_{t=1}$. The accuracy of these data is only about 1% but the lack of agreement between theory and experiment is again striking. Not only is the magnitude of the shift wrong, but the direction of the shift is opposite that predicted by theory. Nowhere over the entire resistivity range is there any consistency between theory and experiment.

IV. DISCUSSION

This experimental investigation shows that the present weak coupling anisotropy theory of superconductivity does not explain the observed behavior of either T_c or H_c in the InTl alloy system. The reasons for the discrepancy are difficult to specify at the present time since data and theory have been compared on only a few alloy systems. More experimental data on other alloy systems are needed if a clue to the mechanism responsible for the departure from theory is to be found.

The T_c and H_c behavior of alloy systems with Sn as a host are well described by anisotropy theory²⁷; but other alloy systems with hosts different from Sn are not as well described. In their paper, MK analyzed alloys with Al and with In as the host metal. In both of these systems they found it necessary to make large changes in the parameter α^i , from impurity to impurity, to achieve consistent fits to theory. As demonstrated in this paper, the choosing of $\alpha^i = 0.4$ in the InTl system now appears unjustified. It would be interesting to see if other alloy systems which were given small values of α^i also show suspicious behavior upon a more detailed ex-

perimental investigation.

To our knowledge, comparisons of experimental results to Clem's critical-field predictions have been reported on only four alloy systems. Three of these were with Sn as a host²⁷ and gave good agreement with predictions while the fourth is the work presented here with In. Another unpublished investigation using In as a host with Sn impurities has been performed by Blech and Serin.²⁸ They noticed a deviation from Clem's \bar{H}_0 predictions which is similar to that found in the present work.

This observed similarity in \bar{H}_0 behavior for two differently doped-In alloys suggests that the deviations may be due to a property of In alone. Clem has suggested that strong coupling effects (i. e., *large electron-phonon* interaction) in In may account for deviations from the weak coupling anisotropy theory. Strong coupling effects are not unexpected in In or in Sn since the electron-phonon interaction in both elements is intermediate between the strong coupling superconductors (e. g., Pb, Hg) and the weak coupling superconductors (e. g., Al, Cd).²⁹ Broadening of the phonon spectrum, as a result of alloying or other means, tends to reduce T_c of a pure superconductor²⁹ and may cause the observed discrepancy from anisotropy theory. However, both the abrupt onset of the discrepancy in In alloys and the lack of a similar discrepancy in Sn alloys remains perplexing.

Clearly there is a need for further experiments to elucidate the problem. The InGa alloy system might give some valuable information since it is in all ways identical to InTl except for the mass and size of the impurity atom. Alloy systems with Pb as a host might also be useful. Pb is known to be a strong superconductor, and therefore strong coupling effects in anisotropy theory might be studied.

ACKNOWLEDGMENT

We are pleased to acknowledge the valuable assistance and advice provided by D. G. Hamblen during the course of this work.

*Work supported in part by the Advanced Research Projects Agency under Contract SD-131, and in part by the U. S. Army Research Office (Durham).

¹Present address: U. S. Naval Research Laboratory, Code 6453G, Washington, D. C. 20390.

¹J. W. Stout and L. Guttman, Phys. Rev. **88**, 703 (1952).

²E. A. Lynton, B. Serin, and M. Zucker, J. Phys. Chem. Solids **3**, 165 (1957).

³G. Chanin, E. A. Lynton, and B. Serin, Phys. Rev. **114**, 719 (1959).

⁴R. A. Connell, Phys. Rev. **129**, 1952 (1963).

⁵M. F. Merriam, J. Hagen, and H. L. Luo, Phys. Rev. **154**, 424 (1967).

⁶D. M. Ginsberg, Phys. Rev. **136**, A1167 (1964).

⁷D. M. Ginsberg, Phys. Rev. **138**, A1409 (1965).

⁸P. W. Anderson, J. Phys. Chem. Solids **11**, 26 (1959).

⁹D. Markowitz and L. P. Kadanoff, Phys. Rev. **131**, 563 (1963).

¹⁰J. R. Clem, Phys. Rev. **153**, 449 (1967).

¹¹R. H. Sherman, S. G. Sydorak, and T. R. Roberts, J. Res. Natl. Bur. Std. (U. S.) **68A**, 579 (1964).

¹²F. G. Brickwedde, H. van Durieux, J. R. Clement,

and J. K. Logan, *J. Res. Natl. Bur. Std. (U. S.)* **64A**, 1 (1960).

¹³D. U. Gubser and D. E. Mapother, *Rev. Sci. Instr.* **40**, 843 (1969).

¹⁴J. M. Ziman, *Electrons and Phonons* (Oxford U. P., Oxford, England, 1963), p. 337.

¹⁵B. B. Goodman, *IBM J. Res. Develop.* **6**, 63 (1962).

¹⁶D. Saint-James and P. G. de Gennes, *Phys. Letters* **7**, 306 (1963).

¹⁷L. J. Barnes and H. J. Fink, *Phys. Letters* **20**, 583 (1966).

¹⁸L. J. Barnes and J. J. Fink, *Phys. Rev.* **149**, 186 (1966).

¹⁹J. Mochel (private communication).

²⁰D. K. Finnemore and D. E. Mapother, *Phys. Rev.* **140**, A507 (1965).

²¹H. R. O'Neal and N. E. Phillips, *Phys. Rev.* **137**, A748 (1965).

²²C. A. Bryant and P. H. Keesom, *Phys. Rev.* **123**, 491 (1961).

²³M. F. Merriam, *Rev. Mod. Phys.* **36**, 152 (1964).

²⁴R. W. Meyerhoff and J. F. Smith, *Acta Met.* **11**, 529 (1963).

²⁵J. A. Rayne, *Phys. Rev.* **129**, 652 (1963).

²⁶N. W. Ashcroft and W. E. Lawrence, *Phys. Rev.* **175**, 938 (1968).

²⁷F. V. Burckbuchler, D. Markowitz, and C. A. Reynolds, *Phys. Rev.* **175**, 543 (1968).

²⁸B. Serin (private communication).

²⁹J. W. Garland, K. H. Bennemann, and F. M. Mueller, *Phys. Rev. Letters* **21**, 1315 (1968).

PHYSICAL REVIEW B

VOLUME 2, NUMBER 7

1 OCTOBER 1970

Theory of Electron Spin Resonance in Type-I Superconductors*

Koya Aoi and James C. Swihart

Department of Physics, Indiana University, Bloomington, Indiana 47401

(Received 1 June 1970)

In order to determine whether electron spin resonance in type-I superconductors is experimentally possible, we have extended Dyson's theory to the case of a superconductor, taking into account the penetration depth of electromagnetic fields, the change in phase of the surface impedance, and the change in group velocity and relaxation time of the quasiparticles compared to the normal case. We have calculated line shapes and magnitudes of power absorbed and rf field transmitted for various frequencies and temperatures for thin-film superconductors. From our calculation, we determine the optimum temperatures and frequencies, and conclude that even for these conditions, the experiment would be difficult.

I. INTRODUCTION

Three years ago Schultz and co-workers¹ observed conduction electron spin resonance (CESR) in normal aluminum, the first such observation in a metal which undergoes a superconducting transition. Hence, the possibility of observing CESR in the superconducting state was raised. If CESR is observed in a superconductor, we might be able to obtain a key to the spin relaxation mechanism in metals. Below 25 °K, the spin relaxation time U in normal Al was found to be temperature independent and values for U were essentially the same for different samples with different resistivity ratios. This leaves the possibility of other mechanisms besides impurity scattering and spin-lattice interactions.¹ Kaplan² calculated the shape of CESR absorption curves for superconducting films of thickness less than or the order of the penetration depth λ by using a phenomenological modified Bloch equation. He concluded that CESR should be observable in the superconducting state. Here we extend Dyson's theory^{3,4} to the case of a thin-film Bardeen-

Cooper-Schrieffer (BCS) superconductor, taking into account changes in the diffusion and spin relaxation of the quasiparticles in the superconducting state. We have calculated not only the line shapes, but also the magnitudes of the power absorbed and rf fields transmitted. We give the temperature and frequency regions for which the resonance will be the largest, and we find that even in the optimum region the resonance will be difficult to observe experimentally.

We consider a film of thickness L parallel to the y - z plane and with surfaces at $x = -\frac{1}{2}L$ and $+\frac{1}{2}L$. A static magnetic field H_0 is applied in the z direction. The linearly polarized rf with its magnetic field H_1 in the y direction will be considered for two situations. (a) The rf field impinges on the film from the negative x region. In this case we shall be interested in the power transmitted through the film into the positive x region. (b) The rf field is set up on both sides of the film with $H_1(\frac{1}{2}L) = H_1(-\frac{1}{2}L)$. In this case we are interested in the power absorbed in the film. We shall refer to these cases as (a) and (b), respectively. Both cases are used experimentally.^{1,5}